Microsecond-Pulsed Dielectric Barrier Discharge Plasma-Treated Mist for Inactivation of Escherichia coli *In Vitro*

Pietro Ranieri, III, Gerard McGovern, Henry Tse, Alexander Fulmer, Mykola Kovalenko, Gary Nirenberg, Vandana Miller, Alexander Fridman, Alexander Rabinovich, and Gregory Fridman

***Abstract*— In this paper, we demonstrate a plasma misting system capable of inactivating *Escherichia coli* O157:H7 (*E.coli*) in a 4 ft^3 (approximately 100 L) volume with potential for future use in decontaminating fresh produce. Water droplets, with an average diameter of 5 μm, are generated via ultrasonic nebulizers and carried by compressed air. These micrometer-sized droplets flowthrough a set of three cylindrical, microsecond-pulsed dielectric barrier discharges (DBDs). We observe the Coulombic fission of droplets up to a critical radius into submicrometer droplets (Sauter mean of approximately 0.3 μm), measured by a laser diffraction analyzer. *E.coli*, on agar plates, is inactivated by this mist in a time and flowrate-dependent manner. We hypothesize that the observed antimicrobial effect correlates with the concentration of submicrometer droplets. The observed formation of submicrometer droplets from this volumetric DBD is similar to the bursting of droplets observed with electrospray devices using corona discharges.**

***Index Terms*— Dielectric barrier discharge (DBD), plasma agriculture, plasma disinfection, plasma misting, pulsed plasma.**

I. Introduction

FOOD-BORNE illnesses due to cross-contamination of produce and wash water by antibiotic-resistant organisms and biofilms present a global challenge for food safety [1]–[3]. Currently, chemical sanitizers and disinfectants are used to reduce microbial growth in wash water up to 5 logs, with increased efficacy if multiple treatments are combined [4]–[6]. Common limitations of these sterilization agents are long treatment times, produce degradation at high concentrations required for disinfection, and overall cost when considering adaptability for industrial application [5].

A nonchemical and nonthermal technology considered for the sterilization and biodecontamination of fresh produce is nonthermal plasma (NTP) due to its potent antimicrobial properties [7]–[13]. NTP may be directly applied for treatment of pathogens on produce or indirectly by modifying washing liquids prior to sterilizing produce [7], [8], [13]–[18]. Although direct treatment via dielectric barrier discharges (DBDs) or atmospheric pressure plasma jets inhibits more microbial growth than indirect treatment, it is often technically complicated to implement at industrial scale, especially on the surface of fresh produce [19]–[24]. Thus, indirect treatment methods may provide a more relevant solution. Reactive oxygen and nitrogen species (RONS), in combination with acids generated in plasma, are the primary factors for sterilization for both indirect and direct plasma treatments [25], [26]. For the indirect inactivation of pathogenic organisms, plasma treatment of liquids before application allows for the accumulation of RONS and reduction in pH. Examples of these systems are bulk water plasma treatments, electrosprays, and flowing water systems [7], [17], [27].

Prior to consumption, all fresh produce must be washed. Current technologies utilize bulk washing of produce in large volumes of water with the addition of active chemicals such as hydrogen peroxide and sodium hypochlorite [28]. As the microbial burden in this water increases so does the incidence of cross-contamination. To minimize the generation of large reservoirs of contaminated liquids, the industry is transitioning toward usage of misting systems that contain high concentrations of antimicrobial agents, but they utilize significantly smaller volumes of liquid to coat the surface of produce in bulk [29], [30]. Standard misting nozzles produce 50–100-μm sized droplets, which causes uneven distribution on produce surface resulting in patchy discoloration of the treated produce. This could also suggest uneven disinfection. This could be addressed by decreasing the droplet size.

In this paper, we present a plasma-based method of generation of droplets with a mean diameter of 0.3 μm. In addition, plasma eliminates the need for added chemical disinfectants

Manuscript received March 2, 2018; revised July 9, 2018; accepted August 28, 2018. Date of publication November 16, 2018; date of current version January 8, 2019. This work was supported by the Improved Processing Technologies (A4131) through the USDA-NIFA Program on Enhancing Food Safety under Grant 2015-68003-23411. The review of this paper was arranged by Senior Editor J. L. Lopez. *(Corresponding author: Pietro Ranieri III.)*

P. Ranieri, III is with the Mechanical Engineering and Mechanics Department, Drexel University, Philadelphia, PA 19104 USA, and also with the Nyheim Plasma Institute, Drexel University, Camden, NJ 08103 USA (e-mail: pjr92@drexel.edu).

G. McGovern was with the Nyheim Plasma Institute, Camden, NJ 08103 USA. He is now with the Department of Chemical Engineering, Drexel University, Philadelphia, PA 19104 USA (e-mail: gjm73@drexel.edu).

H. Tse was with the Nyheim Plasma Institute, Camden, NJ 08103 USA. He is now with the Department of Electrical Engineering, Drexel University, Philadelphia, PA 19104 USA (e-mail: hkt27@drexel.edu).

A. Fulmer was with the Nyheim Plasma Institute, Camden, NJ 08103 USA. He is now with the Department of Materials Science and Engineering, Drexel University, Philadelphia, PA 19104 USA (e-mail: awf28@drexel.edu).

M. Kovalenko, G. Nirenberg, V. Miller, A. Fridman, A. Rabinovich, and G. Fridman are with the Nyheim Plasma Institute, Drexel University, Camden, NJ 08103 USA (e-mail: mk3436@drexel.edu; gn47@drexel.edu; vmiller@coe.drexel.edu; ar483@drexel.edu; af55@coe.drexel.edu; gf33@drexel.edu).

Color versions of one or more of the figures in this paper are available online at http://ieeexplore.ieee.org.

Digital Object Identifier 10.1109/TPS.2018.2878971

0093-3813 © 2018 IEEE. Personal use is permitted, but republication/redistribution requires IEEE permission.
See http://www.ieee.org/publications_standards/publications/rights/index.html for more information.

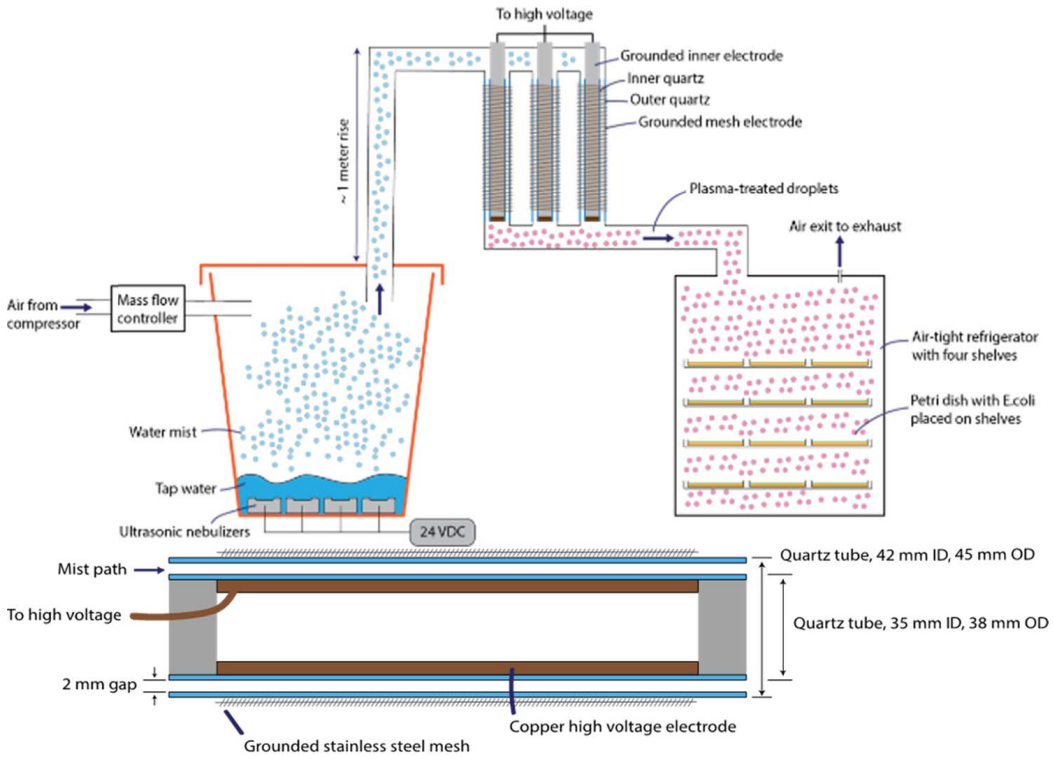


Fig. 1. Schematic of the plasma misting setup and mspDBD electrodes.

by generating RONS as the droplets pass through a plasma. The advantages of treating droplets over bulk water treatments that may contribute to the strong antimicrobial effects are as follows.

1) Submicrometer-to-micrometer-sized water droplets ($d < 20\ \mu$m) suspended in air (mist) can freely move together with the flow of air: viscosity of air can effectively oppose gravity for droplets of this size.
2) The droplet radius is small; thus, the effective surface area is large, facilitating the diffusion of charged and reactive species into the droplet [31].

We present quantitative results on a 100-L system utilizing microsecond-pulsed DBD (mspDBD) for treatment of mist. We observed partial growth inhibition of *Escherichia coli* O157:H7 (*E.coli*) when exposed to plasma-treated mist for up to 30 min. Compared to hurdle technologies that require up to 40 min of treatment for minimally processed produce, the treatment time is competitive [32], [33].

II. Methods

A. Mist Droplet Size Distribution Measurements

Mist droplet size was measured using a laser diffraction droplet size analyzer (Malvern Instruments, USA). The analyzer operated at 10 kHz and averaged an output of 10 000 measurements per second, using a 5-mW He–Ne laser, 10 mm diameter, with a Fourier lens and a detector array to capture the diffracted light. The refractive index for water was used to calculate the size of the water droplets from the diffracted light. Analysis of the particle size distributions was done using the Spraytec 3.30 software (Malvern Instruments, USA) and MATLAB 2016a (MathWorks, USA). The airflow was set to 50 standard liters per minute (SLPM) for all measurements with the droplet analyzer to attain accurate, stable readings for both treated and untreated droplets. At 25 SLPM, the lower flowrate used for antimicrobial assays, the measurement was not accurate.

B. mspDBD Plasma Treatment of Mist

The mspDBD power supply used in these experiments was previously described in detail by Fridman *et al.* [34]. We apply 26-kV pulses at 3500 Hz with 100% duty cycle to three concentric electrodes. These pulses have a 5-kV/ns^{-1} rise time, 2-μs pulse duration, and are single-polarity positive [35], [36]. A general schematic of the plasma treatment and a schematic of the discharge electrode are shown in Fig. 1. Approximately 2.5 cm of tap water covered 14 ultrasonic nebulizers (Model 241V, Sonaer Ultrasonics, USA and powered by a 24-V_{dc} power supply) for droplet generation inside of the bucket. Compressed air, unfiltered, carried the droplets from the bucket to the plasma discharge at a flowrate of 25–50 SLPM. The droplets were elevated vertically prior to entering the electrodes, to remove sufficiently large droplets affected by gravity. We used three identical DBD electrodes with the total plasma treatment cross-sectional area roughly equal to the tube used to deliver the mist (approximately 80 cm^2). Thus, there should be no pressure drop or mass flow restriction between the tubes and the discharge zone. Once in plasma, droplets were treated in a 12.5-cm discharge zone and enter the refrigerator through the top inlet. It takes 2–4 min for the plasma-treated mist to fill the 100-L refrigerator at 50 and 25 SLPM, respectively. The approximate power per square centimeter of mspDBDs is 1 W/cm^2 [36]. For this discharge volume, we estimate the discharge power to be 50.25 W.

For treatment at 30 min and approximately 700 mL (the nebulizers need 100 mL/h each), this equates to about 0.036 kWh/L. The cost to run this system in the USA, where the average energy cost is \$0.12/kWh, will be about \$0.004/L. This cost is competitive with other treatment methods like electrolyzed water that is \$0.04/L [37].

C. Preparation of E.coli for Plasma Treatment

Tryptic soy agar (TSA) plates (Hardy Diagnostics, USA) were inoculated with a rifampicin resistant strain of *E.coli* O157:H7 (gift from Dr. N. Nitin, University of California at Davis, Davis, CA, USA, ATCC #700728) prior to treatment. Fresh cultures were prepared as described previously [38], [39]. Briefly, 5 mL of Bacto tryptic soy broth (Becton Dickinson and Company, USA) containing 25 μL of 10 mg $\cdot$ mL^{-1} rifampicin (Sigma Aldrich, USA) was inoculated with 25 μL of *E.coli* suspension and incubated overnight at 37 °C. The broth was diluted to 2×10^9 CFU $\cdot$ mL^{-1} by comparison with a MacFarland standard in autoclaved distilled water. Using a cotton swab, *E.coli* from this broth was plated on TSA plates using the lawn spread technique on TSA plates containing 0.5 mg $\cdot$ mL^{-1} rifampicin. An antibiotic-resistant strain was chosen because the misting chamber is not operated under sterile conditions. Potential cross-contamination from environmental bacteria could confound the results. This allowed us to investigate the antimicrobial activity of plasma-treated mist against the plated strain and concentration of bacteria.

D. mspDBD Plasma-Treated Mist Treatment of E.coli

E.coli plated from a broth at 10^9 CFU $\cdot$ mL^{-1} was treated with mspDBD plasma-treated mist for up to 30 min at flowrates of 25 or 50 SLPM. Each individual experiment had four replicates; experiments at 25 SLPM were run twice and those at 50 SLPM were run once. After treatment, plates were incubated at 37 °C for 18–24 h, and colony-forming unit was counted manually using a digital colony counter (Hanyan Scientific Equipment, South Korea).

E. Statistical Analysis

The mean and standard error of the colony counts and statistical significance (unpaired and nonparametric t-tests) were calculated using the GraphPad Prism.

III. Results

A. Untreated Water Droplets Combine to Form Larger Droplets

The 14 ultrasonic nebulizers generate mist consisting of submicrometer- to micrometer-sized droplets. The initial droplet size distribution according to the manufacturer is given by the following equation, where γ is the surface tension, ρ is the density of water, C is a constant, and f_a is the frequency of the nebulizer:

$$d = C\sqrt[3]{\frac{\gamma}{\rho f_a^2}}. \tag{1}$$

Surface tension is temperature dependent and is given by the following equation [40], where T is the absolute temperature and T_c is the critical temperature for water (647.15 K):

$$\gamma = 235.8\left[1-\frac{T}{T_c}\right]^{1.256}\left[1-0.625\left(1-\frac{T}{T_c}\right)\right]. \tag{2}$$

For water at 20 °C, the surface tension is 72.8 mN $\cdot$ m^{-1}. Substituting this value into (1) with a nebulizer frequency of 2.4 MHz, constant 0.73, and water density of 1000 kg m^{-3}, the initial droplet size distribution is centered about 1.7 μm. Thus, the droplets entering the airflow are submicrometer- to micrometer-sized prior to entering the electrodes. From the nebulizers, where the mist is generated, the airflow carries the droplets vertically filtering any large droplets ($d > 20$ μm) from the distribution. Any droplets below this diameter will move freely with the airflow; since the viscous forces in the flow are three orders of magnitude larger than the gravitational forces. Theoretically, these smaller droplets should enter the electrodes for the plasma treatment.

The size distribution of untreated droplets at the outlet of the electrodes has a Sauter mean diameter of 5 μm with a range from 1 to 20 μm, as shown in Fig. 2(a). This suggests that the droplets generated from the nebulizers flocculate to form larger droplets during transport through the electrodes. As the initial droplets move from the tube and into the electrodes, the cross-sectional area of the flow is reduced by a third across the three DBD electrodes. The reduction in the area causes the velocity to increase leading to more collisions between the droplets at the inlet of the electrode. Furthermore, the merging of the three flows at the outlet of the electrodes may cause the droplets to collide prior to exiting into the refrigerator. The merging of droplets is likely due to these collisions at the inlet and the outlet of the electrodes.

B. mspDBD Plasma Reduces the Diameter of Smaller Droplets

The water droplet size distribution was measured over time, as shown in Fig. 2(g). The laser transmission (red line), the median diameter (teal line), the Sauter mean diameter (purple line), and the 50% volume fraction diameter (blue line) were recorded and averaged over 10 000 readings per second. The Sauter mean diameter is reduced after treatment with mspDBD plasma. Once the discharge started (denoted by the jump in transmission from below 25% to over 75%), it took approximately 2 min for the reading to stabilize. At this point, the Sauter mean, median, and 50% volume fraction diameter are reduced and stay about constant. The distribution is changed from unimodal to bimodal due to mspDBD plasma treatment [Fig. 2(b)]. The droplet diameter of the smaller distribution is between 0.1 and 1 μm and fills about 30% of the total volume droplet distribution.

We hypothesized that the reduction in volume occurred when the repulsive forces due to the surface charges overcame the surface tension forces holding the droplet together. Repulsive forces due to surface charge were previously reported to induce instability in the droplets of electrospray devices, resulting in a Taylor cone formation and Coulombic fission at high applied voltages (greater than 10–15 kV)

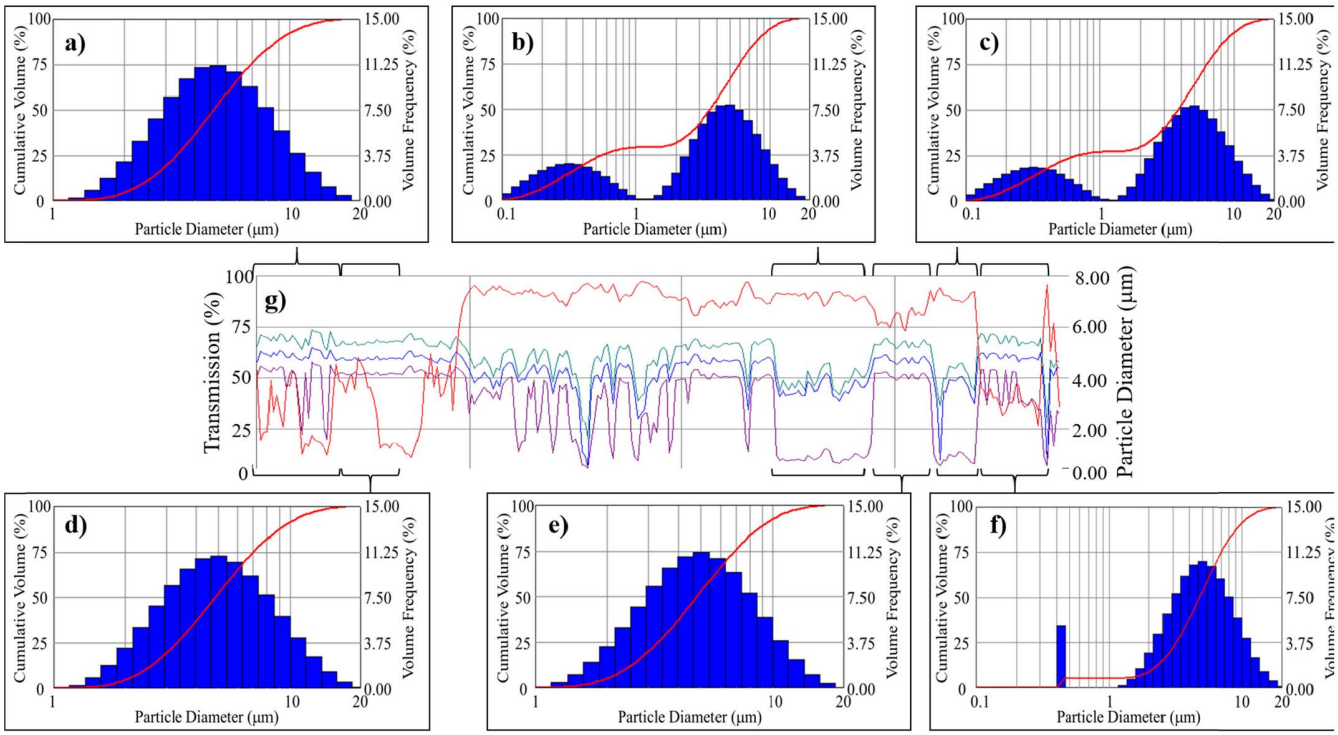


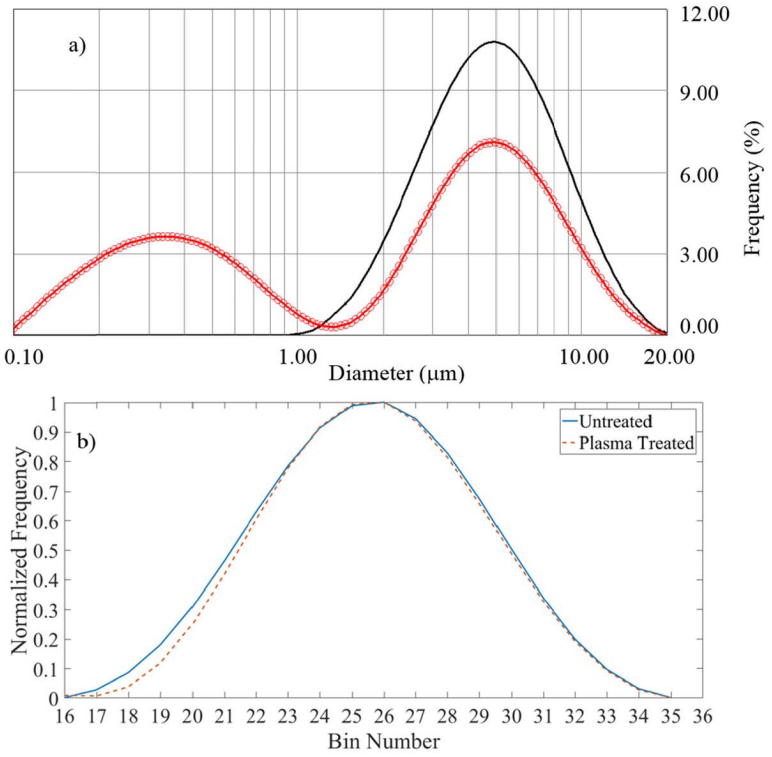
Fig. 2. mspDBD treatment reduces the average size of water droplets. The histogram plots display an x-axis of radii between 0.1 and 20 μm and volume frequency on the y-axis between 0% and 15%. The red line indicates the cumulative volume fraction from 0% to 100%. (a) Particle size distribution of mist at 50 SLPM is a normal distribution centered at 5-μm-diameter droplets. (b) Plasma treatment reduces the average size of the droplets, causing a bimodal distribution with submicrometer droplets. (c) Removal of the grounded mesh reintroduces the submicrometer droplets resulting in the bimodal distribution. (d) Grounded mesh added without plasma treatment did not affect the droplet distribution. (e) Grounded mesh (between the outlet and the detector) was inserted during mspDBD plasma treatment. The submicrometer droplets are removed from the mist restoring the size distribution and frequency comparable to the untreated case. This suggests that all the submicrometer droplets are charged. (f) Plasma was turned OFF and the size distribution returned to a normal distribution. (g) Transmission and distribution chart versus time plot show the transmission of the laser (red line), droplet size median (teal line), Sauter mean (purple line), and 50% volume fraction diameter (blue line) during different treatment parameters.

[41]–[43]. To test if surface charges were responsible for the submicrometer distribution, we inserted a grounded mesh at the outlet of the plasma treatment system to remove the charged droplets from the mist. The histogram of mspDBD treated mist with the grounded mesh Fig. 2(f) is comparable to the control without the plasma Fig. 2(a). This indicates that all the submicrometer droplets are charged and are filtered by the grounded mesh from the mist. When the mesh was removed, the submicrometer droplet population remained in the airflow, and the bimodal distribution was recovered Fig. 2(c). To account for any effects from the grounded mesh itself, untreated droplet sizes were measured with the mesh Fig. 2(e), resulting in the unimodal distribution similar to the control. This indicates that charges are the main contributor to the creation of the bimodal distribution of the plasma-treated mist.

We theorize that the submicrometer droplets (0.1–1 μm in diameter) are formed from Coulombic fission of parent droplets. As shown in Fig. 3(a), the bimodal distribution created by the mspDBD plasma treatment shows an overall reduction of volume frequency of the original unimodal distribution. Coulombic fission due to an applied high voltage is established in the electrospray ionization mass spectrometry and charged aerosol in [41] and [42], [44], [45]. Briefly, when the droplets are exposed to high electric fields, the positive and negative charges within the droplet begin to accumulate at opposite ends. The voltage across the droplet increases with this charge and the effective surface tension of the water decreases. As the electrostatic forces increase to magnitudes comparable to surface tension forces (capillary pressure), the droplet will become unstable at both ends and form Taylor cones. The development of these cones deforms the droplet, which forces the charges to accumulate on the tips of the cone. The size and shape of the deformation are significantly affected by the conductivity of the water with longer shapes at lower conductivity [41]. Eventually, the electrostatic repulsion from surface charges overcomes the surface tension of water, causing them to become unstable and undergo Coulombic fission. The result is the formation of smaller progeny droplets from unstable parent droplets. The critical charge for on the surface of the droplet for the onset of Coulombic fission, known as the Rayleigh stability limit or Coulombic fission limit, is a function of the surface tension and the radius [46], [47]. It is defined as in the following equation [42]:

$$q_R = 8\pi\sqrt{\varepsilon\gamma r_R^3} \tag{3}$$

where q_R is the critical surface charge of the droplet, r_R is the radius of the droplet, and ε is the dielectric constant. The treated droplets will be charged to the floating potential of the discharge, which can be approximated by Bohm's sheath potential, described in the following



c)

Bin Number	Diameter Range (μm)
16	1.0 – 1.16
17	1.16 – 1.36
18	1.36 – 1.58
19	1.58 – 1.85
20	1.85 – 2.15
21	2.15 – 2.51
22	2.51 – 2.92
23	2.92 – 3.41
24	3.41 – 3.98
25	3.98 – 4.64
26	4.64 – 5.41
27	5.41 – 6.31
28	6.31 – 7.35
29	7.35 – 8.57
30	8.57 -10.00
31	10.00 – 11.65
32	11.65 – 13.59
33	13.59 – 15.84
34	15.84 – 18.47
35	18.47 – 21.54
36	21.54 – 25.11

Fig. 3. mspDBD treatment causes Coulombic fission of droplets up to 3.4 μm forming droplets of submicrometer diameter. (a) Untreated distribution (black solid line) and the mspDBD plasma-treated distribution (red circles line) are plotted together. The distribution from 1 to 20 μm diameter is reduced during treatment, which leads to the creation of the bimodal distribution. Plasma treatment reduced the frequency of smaller droplets (less than 5 μm) by a larger amount than larger droplets (greater than 5 μm). This suggests that these smaller droplets burst to create the 0.1–1.0 μm diameter portion of the bimodal distribution. (b) Both 1- and 20-μm distributions from plasma-treated and untreated mist were normalized to their maximums and plotted. Here, we observe that the reduction in frequency begins at bin number 23 (diameters between 2.92 and 3.41 μm), indicating that these are the droplets undergoing Coulombic fission. (c) Droplet diameter range of each bin.

equation [31], [48]:

$$V = \frac{kT_e}{e} \ln\left(\frac{M_i}{2\pi m_e}\right) \tag{4}$$

where V is the floating potential, k is Boltzmann's constant, e is the elementary charge, T_e is the electron temperature, M_i is the mass of ions, and m_e is the mass of an electron. The collected charge on the surface is described by the floating potential and the capacitance of the droplet

$$C = 4\pi\varepsilon r_R \tag{5}$$

$$CV = q_r \tag{6}$$

$$4\pi\varepsilon r_R \frac{kT_e}{e} \ln\left(\frac{M_i}{2\pi m_e}\right) = 8\pi\sqrt{\varepsilon\gamma r_R^3}. \tag{7}$$

We can solve for the critical radius, below which the droplet will burst into smaller droplets creating the observed submicrometer distribution [47]

$$r_R = \frac{1}{4}\frac{\varepsilon}{\gamma}\left(\frac{kT_e}{e} \ln\left(\frac{M_i}{2\pi m_e}\right)\right)^2. \tag{8}$$

For an electron temperature of 3 eV and surface tension of 72.8 mN $\cdot$ m^{-1}, the critical radius of a water droplet is 1.65 μm. This is in good agreement with our observed findings. The droplet size reduction is more prominent on smaller droplets as shown in the normalized distribution in Fig. 3(b). Here, the onset diameter of Coulombic fission is between 2.9 and 3.4 μm, corresponding to radius sizes of 1.45–1.7 μm, respectively. Therefore, droplets up to approximately 1.7 μm in diameter are susceptible to Coulombic fission during the mspDBD plasma treatment in this system. As shown in (8), the critical radius, here, is inversely proportional to the surface tension of the liquid. This suggests that for liquids with large conductivities, the critical radius will be smaller. We used tap water in experiments, which may result in different critical radii of other experiments due to the variation of conductivity between water sources.

The size distribution of the submicrometer charged droplets is relatively uniform at the outlet of the discharge. This indicates that the smaller droplets are stable and the distributed charge from the parent droplet does not surpass the fission limit. It was previously reported that the distributed charge among the progeny droplets is about 0.7$\times$ their limit [49]. The progeny droplets have a radius smaller by an order of magnitude, thus their critical charge is about 30$\times$ less than the parent droplet and should be more prone to fission. However, due to their stability at the outlet of the discharge, the surface tension force on the smaller droplets must be greater than the repulsive force. The relationship between the critical radius and the critical charge as described in (3) shows that both forces are dependent on the radius. They can be written to be approximately

$$F_{\text{repulsion}} \approx \frac{q^2}{r^2} \tag{9}$$

$$F_{\text{tension}} \approx \gamma r. \tag{10}$$

Here, the repulsion force and the tension force are inversely and linearly related to the radius, respectively. These forces are equal the moment prior to fission, where the charge is comparable to the critical charge. Once fission occurs, the critical charge is distributed across all progeny droplets. The reduction in charge is proportional to the reduction in volume, ($q \approx r^3$), thus

$$F_{\text{repulsion}} \approx \frac{r^6}{r^2} \approx r^4. \tag{11}$$

Therefore, the reduction in volume due to fission significantly reduces the repulsion force when compared to surface tension. This indicates that offspring droplets of smaller radii are stabilized outside of the discharge. In contrast, the parent droplets with larger radii have a higher charge and are more susceptible to fission.

C. mspDBD Treated Mist Inhibits the Growth of E.coli

Our previous reports showed that the mspDBD plasma-treated mist inactivates *E.coli* on TSA plates using a single concentric DBD, consisting of a cylindrical high-voltage electrode encased in a grounded metal electrode [13]. For this paper, we built a larger treatment system able to accommodate higher flowrates of mist while retaining its antimicrobial efficacy. To test this, *E.coli* plated on TSA plates was treated for 30 min at 50 SLPM and compared to untreated control cultures. *E.coli* plates were placed on different shelves (Fig. 1); the shelf closest to the inlet of the plasma-treated mist is labeled #1 and the furthest at the base of the refrigerator as #4. As shown in Fig. 4, plasma-treated mist partially inhibited *E.coli* growth when compared to the untreated control. Based on our previous work, the efficacy of the treated mist is attributed to the RONS that solvate into the droplets during plasma treatment [13]. Therefore, the antimicrobial activity may be dependent on the concentration of the plasma-generated reactive species inside the droplets.

D. Longer Plasma Residence Time Increases Antimicrobial Efficacy

We tested the effect of plasma residence time on antimicrobial efficacy by changing the carrier gas flowrate as shown in Table I. We observed an average of 2500 colonies grown at 50 SLPM under our experimental conditions of applied voltage of 26 kV, frequency of 3500 Hz, and 30-min treatment time; and averages of 40 and 425 colonies at 25 SLPM at treatment times of 30 and 15 min, respectively. Longer treatment times and lower flowrates produce a statistically significant change in antimicrobial efficacy of the mist. As shown in Fig. 4, similar magnitudes of inactivation were observed across all shelves, indicating adequate mixing in the refrigerator. These observations combined suggest that the antimicrobial activity of the droplets is directly related to the plasma residence time. The doubling of residence time allows more droplets to reach the fission limit, forming a higher population of submicrometer charged droplets. In addition, it allows for a higher concentration of gas-phase plasma-generated RONS to solvate into the droplet during transport through the plasma. Future work will determine the RONS concentration in the droplet after plasma treatment and the flux of species to the bacteria.

IV. Discussion

Our previous studies showed antimicrobial activity against *E.coli* using a single DBD to generate mspDBD plasma-treated mist [13]. For industrial scale sterilization of fresh produce, these misting systems require a larger treated volume of mist and the ability to disinfect all surfaces of the produce. To address these issues, the present device uses a misting system able to treat approximately 100 L, accommodates flowrates up to 50 SLPM, and can treat any shape of produce.

We hypothesize that the strong antimicrobial effect of the plasma-treated mist correlates with the concentration of charged, submicrometer droplets. In addition, the water droplets serve as the key source of hydrogen in this paper and allow for the formation of OH radicals and H_2O_2, the key effectors of pathogen inactivation [1]. The increased RONS diffusion into the droplet facilitated by droplet's larger surface area to volume ratio may be a contributor to the antimicrobial effect [31], [50]. In addition, the reduced volume of the droplet causes enhanced mixing of the RONS within the droplet. On the other hand, the plasma-generated ions solvate on their own, and neutrals will follow Henry's Law with solvated concentration increasing with residence time [51]. The concentration and identification of RONS in the droplet will be studied in the future work. Since this paper was performed using tap water (conductive liquid is needed for the ultrasonic nebulizers), the role of chlorates, perchlorate, and other dissolved ions and minerals also needs to be examined to evaluate their contribution in the antimicrobial effect of the mist.

In this paper, we demonstrate that mspDBD plasma produces smaller droplets from large drops and inhibits the growth of microbes. Similar effects were observed when utilizing a corona discharge to generate an electrospray for the treatment of suspended microbes and biofilms [7], [8], [52]. The volumetric DBD treatment of mist has some advantages over electrospray treatment systems.

1) Higher applied voltages that cause the accumulated surface charge to reach the fission limit.
2) Both, parent and progeny droplets (formed after Coulombic fission of the former) continued to be exposed to plasma discharge after fission.
3) Simultaneous treatment of droplets of multiple sizes, as the treated droplet is limited to the capillary tube diameter in electrospray devices.

Both, electrospray and mspDBD treated droplets may be more effective than industry standard methods for the sterilization of fresh produce as the droplets are smaller than those currently utilized in standard misting nozzles. Furthermore, these treatments may inhibit microbial growth above the industry standard of three logs [7], [28].

The progeny droplets will undergo Coulombic fission themselves if they are generated inside the discharge. The radii and critical charge of the progeny droplets are a 10th and a 30th, respectively, of the parent droplets, therefore, there is enough charge deposition to cause fission of the progeny droplets in

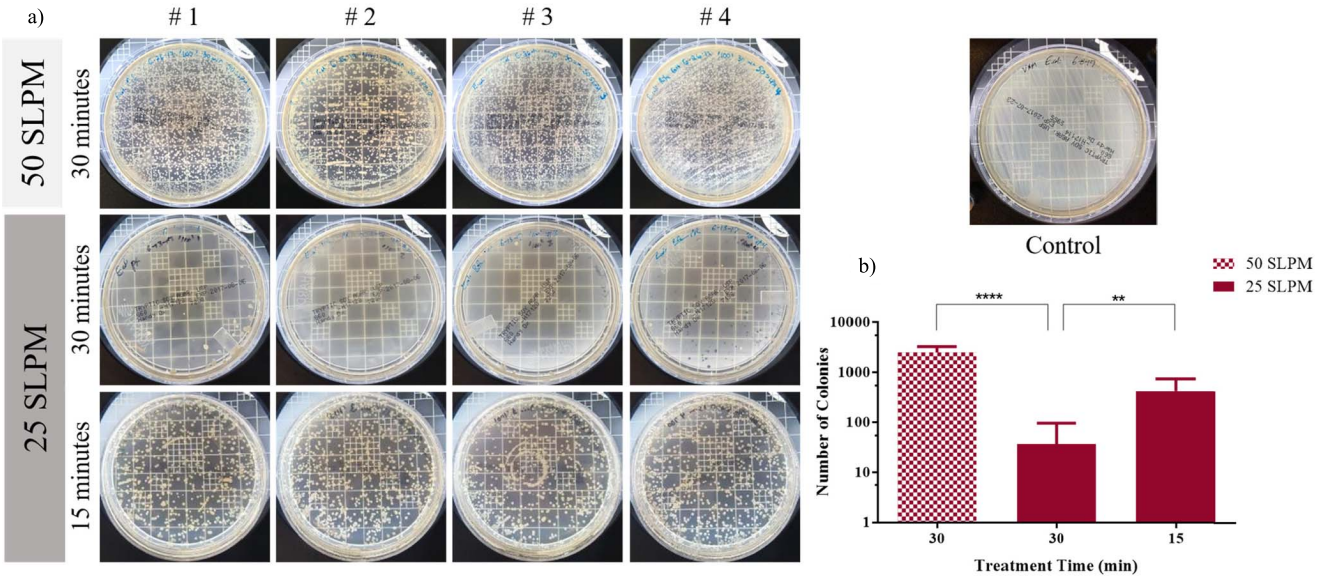


Fig. 4. mspDBD treated mist inactivates *E.coli* in a time and flowrate-dependent manner. (a) Inoculated plates were placed on top-to-bottom shelves, #1–4, prior to exposure to plasma-treated mist. After exposure to plasma-treated mist for 30 min at 50 SLPM, an average of 2500 colonies grew on the plates (top row). When the flowrate was reduced to 25 SLPM, the number of remaining colonies was reduced to an average of 40 (middle row). This indicates that longer plasma residence time produces a mist with a stronger antimicrobial effect. A reduced effectiveness was observed when the treatment time was decreased to 15 min (average of 425 colonies) (bottom row). (b) Colonies remaining after treatment at different times and different flowrates. $^{****}p < 0.0001$, $^{**}p < 0.004$.

the discharge. As the droplets travel through the plasma, they gain thermal energy, causing increased evaporation rate than from the airflow alone [53]. The reduction in diameter due to evaporation will cause the submicrometer–micrometer-sized droplets to be more susceptible to Coulombic fission while in the plasma discharge zone. The minimum droplet size will be reached when the formation of water clusters is favored over droplets. Although our data would suggest this to be 0.1 μm in diameter (the smallest measured diameter of the submicrometer droplets), it is the detection limit of the droplet analyzer we utilized for this paper. Therefore, there may be droplets smaller in diameter in the plasma-treated mist; this remains to be studied. Due to the limitations of our detection systems, we were unable to study the relationship between the increased plasma residence time and concentration of submicrometer droplets as the mist diffuses away from the detector at this flowrate. This will be addressed in the future work to determine the dependence of submicrometer droplets on plasma residence time.

V. Conclusion

This paper shows the antimicrobial efficacy of mspDBD treated mist for disinfection in an industrial setting. The proposed mechanism for the observed strong antimicrobial efficacy of plasma-treated mist is the formation of submicrometer droplets with large concentrations of reactive species. In comparison to the parent droplets, these smaller progeny droplets have greater diffusion of plasma-generated RONS into the droplet. Furthermore, there is enhanced mixing in the droplet due to the reduced volume. Future work will focus on inactivating pathogens on produce with the mspDBD treated mist while leaving the produce unaffected. In addition, the dependence on plasma residence time of the chemical composition in the droplets and the formation of the submicrometer droplets will be investigated.

Acknowledgment

P. Ranieri would like to thank J. Wolfgang (Malvern Instruments) for his advice and assistance for interpretation of the droplet size measurement data.

References

[1] J. L. Banach, I. Sampers, S. Van Haute, and H. J. Van der Fels-Klerx, "Effect of disinfectants on preventing the cross-contamination of pathogens in fresh produce washing water," *Int. J. Environ. Res. Public Health*, vol. 12, no. 8, pp. 8658–8677, 2015.

[2] I. K. Jahid and S.-D. Ha, "A review of microbial biofilms of produce: Future challenge to food safety," *Food Sci. Biotechnol.*, vol. 21, no. 2, pp. 299–316, 2012.

[3] C. Potera, "Forging a link between biofilms and disease," *Science*, vol. 283, no. 5409, pp. 1837–1839, 1999.

[4] K. Joshi, R. Mahendran, K. Alagusundaram, T. Norton, and B. K. Tiwari, "Novel disinfectants for fresh produce," *Trends Food Sci. Technol.*, vol. 34, no. 1, pp. 54–61, 2013.

[5] C. Goodburn and C. A.Wallace, "The microbiological efficacy of decontamination methodologies for fresh produce: A review," *Food Control*, vol. 32, no. 2, pp. 418–427, 2013.

[6] E. Petri, M. Rodríguez, and S. García, "Evaluation of combined disinfection methods for reducing *Escherichia coli* O157:H7 population on fresh-cut vegetables," *Int. J. Environ. Res. Public Health*, vol. 12, no. 8, p. 8678, 2015.

[7] Z. Machala, B. Tarabova, K. Hensel, E. Spetlikova, L. Sikurova, and P. Lukes, "Formation of ROS and RNS in water electro-sprayed through transient spark discharge in air and their bactericidal effects," *Plasma Process. Polym.*, vol. 10, no. 7, pp. 649–659, 2013.

[8] Z. Machala, L. Chládeková, and M. Pelach, "Plasma agents in bio-decontamination by dc discharges in atmospheric air," *J. Phys. D: Appl. Phys.*, vol. 43, no. 22, p. 222001, 2010.

[9] P. J. Bruggeman *et al.*, "Plasma–liquid interactions: A review and roadmap," *Plasma Sour. Sci. Technol.*, vol. 25, no. 5, p. 053002, 2016.

[10] O. Schlüter *et al.*, "Opinion on the use of plasma processes for treatment of foods," *Mol. Nutrition Food Res.*, vol. 57, no. 5, p. 920, 2013.

[11] J. Guo, K. Huang, and J. Wang, "Bactericidal effect of various non-thermal plasma agents and the influence of experimental conditions in microbial inactivation: A review," *Food Control*, vol. 50, pp. 482–490, Apr. 2015.
[12] V. Scholtz, J. Pazlarova, H. Souskova, J. Khun, and J. Julak, "Nonthermal plasma—A tool for decontamination and disinfection," *Biotechnol. Adv.*, vol. 33, no. 6, pp. 1108–1119, 2015.
[13] K. Patel *et al.*, "Mechanisms of biocidal activity of dielectric barrier discharge air jet with misting," *Plasma Med.*, vol. 6, nos. 3–4, pp. 447–457, 2016.
[14] S. C. Min *et al.*, "Inactivation of *Escherichia coli* O157:H7 and aerobic microorganisms in romaine lettuce packaged in a commercial polyethylene terephthalate container using atmospheric cold plasma," *J. Food Protection*, vol. 80, no. 1, pp. 35–43, 2017.
[15] A. Patange, D. Boehm, C. Bueno-Ferrer, P. J. Cullen, and P. Bourke, "Controlling *Brochothrix thermosphacta* as a spoilage risk using in-package atmospheric cold plasma," *Food Microbiol.*, vol. 66, pp. 48–54, Sep. 2017.
[16] D. Ziuzina *et al.*, "Demonstrating the potential of industrial scale in-package atmospheric cold plasma for decontamination of cherry tomatoes," *Plasma Med.*, vol. 6, nos. 3–4, pp. 397–412, 2016.
[17] P. Lukes, E. Dolezalova, I. Sisrova, and M. Clupek, "Aqueous-phase chemistry and bactericidal effects from an air discharge plasma in contact with water: Evidence for the formation of peroxynitrite through a pseudo-second-order post-discharge reaction of H_2O_2 and HNO_2," *Plasma Sour. Sci. Technol.*, vol. 23, no. 1, p. 015019, 2014.
[18] S. K. Pankaj *et al.*, "Applications of cold plasma technology in food packaging," *Trends Food Sci. Technol.*, vol. 35, no. 1, pp. 5–17, 2014.
[19] M. Cooper, G. Fridman, A. Fridman, and S. G. Joshi, "Biological responses of Bacillus stratosphericus to floating electrode-dielectric barrier discharge plasma treatment," *J. Appl. Microbiol.*, vol. 109, no. 6, pp. 2039–2048, 2010.
[20] S. G. Joshi, M. Paff, G. Friedman, G. Fridman, A. Fridman, and A. D. Brooks, "Control of methicillin-resistant Staphylococcus aureus in planktonic form and biofilms: A biocidal efficacy study of nonthermal dielectric-barrier discharge plasma," *Am. J. Infect. Control*, vol. 38, no. 4, pp. 293–301, 2010.
[21] G. Fridman *et al.*, "Comparison of direct and indirect effects of non-thermal atmospheric-pressure plasma on bacteria," *Plasma Process. Polym.*, vol. 4, no. 4, pp. 370–375, 2007.
[22] J.-S. Chang, "Recent development of plasma pollution control technology: A critical review," *Sci. Technol. Adv. Mater.*, vol. 2, nos. 3–4, pp. 571–576, 2001.
[23] A. Lacombe *et al.*, "Nonthermal inactivation of norovirus surrogates on blueberries using atmospheric cold plasma," *Food Microbiol.*, vol. 63, pp. 1–5, May 2017.
[24] B. A. Niemira, "Targeting biofilms with cold plasma: New approaches to a persistent problem," *Biofilms*, 2017.
[25] D. B. Graves, "The emerging role of reactive oxygen and nitrogen species in redox biology and some implications for plasma applications to medicine and biology," *J. Phys. D: Appl. Phys.*, vol. 45, no. 26, p. 263001, 2012.
[26] M. Laroussi, I. Alexeff, and W. L. Kang, "Biological decontamination by nonthermal plasmas," *IEEE Trans. Plasma Sci.*, vol. 28, no. 1, pp. 184–188, Feb. 2000.
[27] J. Brar *et al.*, "Non-thermal plasma treatment of flowing water: A solution to reduce water usage and soil treatment cost without compromising yield," *Plasma Med.*, vol. 6, nos. 3–4, pp. 413–427, 2016.
[28] M. I. Gil, M. V. Selma, F. López-Gálvez, and A. Allende, "Fresh-cut product sanitation and wash water disinfection: Problems and solutions," *Int. J. Food Microbiol.*, vol. 134, nos. 1–2, pp. 37–45, 2009.
[29] K. Walia *et al.*, "The efficacy of disinfectant misting in the lairage of a pig abattoir to reduce *Salmonella* and *Enterobacteriaceae* on pigs prior to slaughter," *Food Control*, vol. 75, pp. 55–61, May 2017.
[30] L. McCartney and M. Lefsrud, "Portable frost-protection misting system: Trial on tomato and sweet orange crops," *HortTechnology*, vol. 25, no. 3, pp. 313–321, 2015.
[31] A. Fridman, *Plasma Chemistry*. Cambridge, U.K.: Cambridge Univ. Press, 2008.
[32] N. Singh, R. K. Singh, A. K. Bhunia, and R. L. Stroshine, "Efficacy of chlorine dioxide, ozone, and thyme essential oil or a sequential washing in killing *Escherichia coli* O157:H7 on lettuce and baby carrots," *LWT-Food Sci. Technol.*, vol. 35, no. 8, pp. 720–729, 2002.
[33] J. L. Banach, H. van Bokhorst-van de Veen, L. S. van Overbeek, P. S. van der Zouwen, H. J. van der Fels-Klerx, and M. N. Nierop Groot, "The efficacy of chemical sanitizers on the reduction of *Salmonella* Typhimurium and *Escherichia coli* affected by bacterial cell history and water quality," *Food Control*, vol. 81, pp. 137–146, Nov. 2017.
[34] G. Fridman, M. Peddinghaus, M. Balasubramanian, H. Ayan, A. Fridman, and A. Gutsol, "Blood coagulation and living tissue sterilization by floating-electrode dielectric barrier discharge in air," *Plasma Chem. Plasma Process.*, vol. 26, no. 4, pp. 425–442, 2006.
[35] D. Dobrynin, G. Fridman, G. Friedman, and A. Fridman, "Physical and biological mechanisms of direct plasma interaction with living tissue," *New J. Phys.*, vol. 11, no. 11, p. 115020, 2009.
[36] H. Ayan *et al.*, "Heating effect of dielectric barrier discharges for direct medical treatment," *IEEE Trans. Plasma Sci.*, vol. 37, no. 1, pp. 113–120, Jan. 2009.
[37] S. Rahman, I. Khan, and D.-H. Oh, "Electrolyzed water as a novel sanitizer in the food industry: Current trends and future perspectives," *Comprehensive Rev. Food Sci. Food Safety*, vol. 15, no. 3, pp. 471–490, 2016.
[38] A. Cossu, D. Ercan, Q. Wang, W. A. Peer, N. Nitin, and R. V. Tikekar, "Antimicrobial effect of synergistic interaction between UV-A light and gallic acid against *Escherichia coli* O157:H7 in fresh produce wash water and biofilm," *Innov. Food Sci. Emerg. Technol.*, vol. 37, pp. 44–52, Oct. 2016.
[39] E. F. de Oliveira, A. Cossu, R. V. Tikekar, and N. Nitin, "Enhanced antimicrobial activity based on a synergistic combination of sublethal levels of stresses induced by UV-A light and organic acids," *Appl. Environ. Microbiol.*, vol. 83, no. 11, p. 00383, 2017.
[40] N. B. Vargaftik, B. N. Volkov, and L. D. Voljak, "International tables of the surface tension of water," *J. Phys. Chem. Ref. Data*, vol. 12, no. 3, p. 817, 1983.
[41] B. Pongrác, H.-H. Kim, N. Negishi, and Z. Machala, "Influence of water conductivity on particular electrospray modes with dc corona discharge—Optical visualization approach," *Eur. Phys. J. D*, vol. 68, no. 8, p. 224, 2014.
[42] J. N. Smith, R. C. Flagan, and J. Beauchamp, "Droplet evaporation and discharge dynamics in electrospray ionization," *J. Phys. Chem. A*, vol. 106, no. 42, pp. 9957–9967, 2002.
[43] H. H. Kim *et al.*, "Polarity effect on the electrohydrodynamic (EHD) spray of water," *J. Aerosol Sci.*, vol. 76, pp. 98–114, Oct. 2014.
[44] P. D. Maguire *et al.* "Controlled microdroplet transport in an atmospheric pressure microplasma," *Appl. Phys. Lett.*, vol. 106, no. 22, p. 224101, 2015.
[45] J. Q. Xu, D. Balik, and G. R. Agnes, "Aerosol static electrification and its effects in inductively coupled plasma spectroscopy," *J. Anal. Atomic Spectrometry*, vol. 16, no. 7, pp. 715–723, 2001.
[46] K.-Y. Li, H. Tu, and A. K. Ray, "Charge limits on droplets during evaporation," *Langmuir*, vol. 21, no. 9, pp. 3786–3794, 2005.
[47] H. M. A. Elghazaly and G. S. P. Castle, "Analysis of the instability of evaporating charged liquid drops," *IEEE Trans. Ind. Appl.*, vol. IA-22, no. 5, pp. 892–896, Sep. 1986.
[48] G. Fridman, L. Mengyan, P. I. Lelkes, G. Friedman, A. Fridman, and A. F. Gutsol, "Nonthermal plasma bio-active liquid micro and nano-xerography," *IEEE Trans. Plasma Sci.*, vol. 33, no. 3, pp. 1061–1065, Jun. 2005.
[49] I. G. Loscertales and J. Fernández de la Mora, "Experiments on the kinetics of field evaporation of small ions from droplets," *J. Chem. Phys.*, vol. 103, no. 12, p. 5041, 1995.
[50] R. Burlica, K.-Y. Shih, and B. R. Locke, "Formation of H_2 and H_2O_2 in a water-spray gliding arc nonthermal plasma reactor," *Ind. Eng. Chem. Res.*, vol. 49, no. 14, pp. 6342–6349, 2010.
[51] S. Ognier, D. Iya-Sou, C. Fourmond, and S. Cavadias, "Analysis of mechanisms at the plasma–liquid interface in a gas–liquid discharge reactor used for treatment of polluted water," *Plasma Chem. Plasma Process.*, vol. 29, no. 4, pp. 261–273, 2009.
[52] Z. Kovalova, M. Leroy, J. M. Kirkpatrick, E. Odic, and Z. Machala, "Corona discharges with water electrospray for *Escherichia coli* biofilm eradication on a surface," *Bioelectrochemistry*, vol. 112, pp. 91–99, Dec. 2016.
[53] M. M. Iqbal and M. M. Turner, "Investigations of droplet-plasma interaction using multi-dimensional coupled model," *Contrib. Plasma Phys.*, vol. 55, no. 9, pp. 627–642, 2015.

Authors' biographies and photographs not available at the time of publication.